Noble gas incorporation into silicate glasses: implications for planetary volatile storage

Hong Yang[1], Arianna E. Gleason[1,2], Sergey N. Tkachev[3], Bin Chen[4], Raymond Jeanloz[5], Wendy L. Mao[1,2]

[1] Department of Geological Sciences, Stanford University, Stanford, CA 94305, USA

[2] SLAC National Accelerator Laboratory, Menlo Park, CA 94025, USA

[3] Center for Advanced Radiation Sources, University of Chicago, Chicago, Illinois 60637, USA

[4] Center for High Pressure Science and Technology Advanced Research, Pudong, Shanghai 201203, China

[5] Earth and Planetary Sciences Department, University of California, Berkeley, CA 94720, USA

Abstract

Incorporation of small molecules in silicate melts may provide an important mechanism for storing noble gases in the deep Earth, yet the means by which chemically inert noble gases enter and are retained in silica-based materials is not understood. High-pressure, room-temperature sound velocity measurements on silica and natural-basalt glasses in different pressure-transmitting media reveal that neon enters the structure of silicate glasses and enhances their elastic strengths, whereas ethanol-methanol mixture does not. Combined with literature data, we found the incorporation of small molecules into silica and basalt glasses is controlled by the void size distribution of the glass and size of the molecules. Pressure primarily reduces the size of noble gases, thereby increasing their solubilities in silicate melts and glasses.

Introduction

Radiogenic heat production generates ^{40}Ar, ^{21}Ne and ^{4}He inside Earth, and the ratios of these isotopes to non-radiogenic isotopes have been used to infer the style of mantle convection and the source of ocean island basalts (e.g. Mukhopadhyay and Parai, 2019). Owing to their changing reactivity and volatility with pressure, noble gases are also useful geochemical tracers for interior processes of planets (e.g. Sanloup *et al.*, 2005). However, how these noble gases are distributed among potential geochemical reservoirs, and how they alter the physical properties of their host with increasing depth (and therefore pressure) is still unclear. The storage of noble gases in quartz, ferropericlase, and bridgmanite at high pressure has been experimentally verified (Rosa *et al.*, 2020; Sanloup *et al.*, 2005). Nevertheless, the partition coefficients of noble gases between minerals and melts are on the order of 10^{-3} (Karato, 2016), implying significant storage of noble gases in silicate melts. This deep storage could also potentially alter atmospheric composition. As silicate glasses and melts share structural similarities (Morard *et al.*, 2020; Williams and Jeanloz, 1988), with glass being the kinetically hindered state of the corresponding melt, understanding the incorporation of noble gases into silicate glasses can shed light on their storage in natural silicate melts.

Noble gases are widely used as pressure-transmitting media in high-pressure diamond-anvil cell experiments. These gases are chemically inactive and display relatively low mechanical strength, and thus minimize pressure gradients and deviatoric stresses in the sample chamber (Angel *et al.*, 2007; Klotz *et al.*, 2009). Use of noble gases as pressure-transmitting media presumes minimal interaction with the pressurized sample, yet there have been several reports that helium

47 penetrates into the structure of silica glass at room temperature. (Sato *et al.*, 2011; Shen *et al.*,
48 2011; Weigel *et al.*, 2012). These results indicate that helium gets into the structure of silica
49 glass, enhancing both its incompressibility and rigidity. Another study on basalt and enstatite
50 glasses also indicates neon can enter their structure at high pressure (Clark *et al.*, 2016).
51
52 Void-space analysis of silica could shed light on the incorporation of noble gases into its
53 structure. Theoretical simulations of the structure of silica glass and void-size analysis have
54 provided statistics on the interstitial space (i.e., the largest spherical site not occupied by Si or O)
55 that could potentially be available for incorporating noble gases (Malavasi *et al.*, 2006;
56 Shackelford and Masaryk, 1978). Assuming the distribution of the interstitial sites follows a log-
57 normal distribution, Shackelford and co-workers found the highest density of interstitial site
58 diameters at d = 1.81 Å, with the distribution extending to around d = 4.0 Å. Based on this result,
59 the four smaller-sized noble gases, He (d = 2.551 Å), Ne (d = 2.820 Å), Ar (d = 3.542 Å) and Kr
60 (d = 3.655 Å), can occupy some fraction of the interstitial sites in silica glass, and potentially
61 modify the structure and physical properties. Another theoretical structure simulation based on
62 molecular dynamics found an overall smaller void size, suggesting limited incorporation of Ar
63 and larger-sized molecules. However, systematic study of the high-pressure solubility of these
64 gases in silica glass has been lacking, despite a number of studies on helium (Sato *et al.*, 2011;
65 Shen *et al.*, 2011; Weigel *et al.*, 2012).
66
67 To help clarify the mechanism of noble-gas incorporation into amorphous silica and natural
68 silicate glasses, we measured high-pressure Brillouin spectra of silica and basalt glasses using
69 different pressure transmitting media at room temperature. The measured elastic properties of the

material provide insight into the structural evolution and molecule incorporation of each glass with compression. Elasticity is a useful monitor of the solution process because *in situ* measurement of gas solubility is challenging at high pressure. Together with existing literature data, we provide a comprehensive review of noble gases migrating into silica glass and natural basalt glasses under pressure. We find that solubility is controlled by the atomic sizes of the noble gases relative to the size of available interstitial spaces in the silicate glasses. Pressure alters both factors, thereby affecting the solubility of noble gases and other volatile species in glasses and melts. Our results support the potential for increased storage of noble gases in Earth's and other deep planetary interiors.

Results

Details on sample synthesis, compositions, and data collection can be found in the Supplementary Information. We found that the sound velocities of silica glass depend on the pressure-transmitting medium, as measured at pressures ranging from 0-10 GPa (Fig. 1). For both the compressional and shear velocities of silica glass, we observed a drop in velocity when increasing pressure between 1 and 3 GPa, followed by a slightly increasing or nearly unchanged velocity at higher pressures (Fig. 1). Silicate glasses with natural compositions share a similar framework structure with silica glass, and the velocity drop upon initial compression was also documented in other polymerized silicate glasses, such as basalt, jadeite and albite glasses (Liu and Lin, 2014; Sakamaki *et al.*, 2014). In contrast, depolymerized glasses like diopside or enstatite glass do not show a decreasing trend, but rather an almost pressure-independent velocity (Liu and Lin, 2014; Sakamaki et al., 2014; Sanchez-Valle and Bass, 2010). These observations can be explained by the flexibility of SiO_4 tetrahedra networks. In the low-pressure range, below

3 GPa, the SiO_4 tetrahedra in the glass rotate into the void space to form a high-density structure (Clark *et al.*, 2016). The rotation does not involve substantial compression of the interatomic bonds, so the elastic moduli of the material remain largely unaltered. Therefore, the velocities, given by the square root of the ratio of the moduli and density, decreases during this stage.

However, after the void space is filled, tetrahedral rotation is replaced by the interatomic bonds shortening, and the sound velocities then increase under compression (Clark *et al.*, 2016). Depolymerized silicate glasses, which contain larger 'modifier' cations like Mg^{2+}, Na^{2+} or Ca^{2+}, have less void space and consequently less flexibility. The densification may also involve some chemical bond shortening and leads to the unchanged velocity profile with increasing pressure. This explanation is supported by molecular dynamics (MD) simulations on silicate glasses and melts over a wide compositional range (Guillot and Sator, 2007; Salmon *et al.*, 2019), with a decrease in Si-O-Si angle documented between 0-5 GPa.

For basalt glasses, sound velocities at high pressure are also influenced by the pressure media (Fig. 2). The BIR-1 sample has higher velocities in a neon medium, as compared with basalt in M-E and M-E-W (methanol: ethanol: water = 16:3:1); it also has an earlier transition pressure at which the velocities start to increase. Comparing the M-E and M-E-W cases, we see that water seems to lower the decreasing slope below 5 GPa, but it does not change the transition point for the change in velocity trends (Fig. 2). In fact, water enhancing glass incompressibility has been reported (Murakami, 2018) and the velocity difference between the two cases here could be due to water penetration (Fig. 3).

Discussion

Sound velocity data for amorphous materials can be very useful to calculate its density at high pressure (Zha *et al.*, 1994). However, this method would fail if pressure media penetrates the sample (Weigel *et al.*, 2012). We calculated the *P-V* curve from velocities observed in different media and used this to examine whether incorporation of pressure media occurred in our experiments (See Supplementary Information for details). Neon and helium are able to penetrate into the silica structure while water and methanol molecules seem to also be able to penetrate into basalt glasses (Fig. S-3).

We compared the molecular size of the pressure media with the size of the interstitial space in the silica structure (Fig. 3 and S-4). It is found that at ambient conditions, the sizes of helium, neon and water molecules are smaller than some voids in the silica structure. At higher pressures, the void size distribution generally shifts to smaller volume, but the peak position only slightly moves and is still larger than 1.75 Å. On the other hand, the sizes of highly compressible gases decrease dramatically with increasing pressure, especially for helium and neon (Fig. S-4). At 5.7 GPa and 4000 K, almost half of the interstitial sites are open to helium and around 20% are open to neon. These results indicate that helium and neon elevate the elastic stiffness of silica by supporting the structure in the void space, while molecules larger than argon are too big to be incorporated into silica and did not show this effect. Pressure makes these atoms smaller, enhancing the solubility of neon and helium into silica (Fig. 3). Although argon also becomes smaller at high pressure, it is still larger than most of the voids in silica. Its solubility is limited and does not influence the elastic properties significantly (Fig. 1).

Our measurements do not provide solubility values, but by comparing the gas and non-gas experiments we can make an estimate of this number (Sato *et al.*, 2011) (Fig. S-3). In Figure 4, the upper limit is constrained by the maximum available space in the silica structure. This space is calculated as the volume difference between normal silica and the ultra-dense six-coordinated silica extropolated to lower pressure. On the other hand, the lower limit is given by the difference between gas and non-gas curves, assuming the 'expansion' should wholy or partly come from the volume of gas in the structure. Since the partial volume of a component in a mixture is smaller than the volume of its own existence (Bajgain *et al.*, 2015), the real solubility should be higher than the lower limit here.

Basalt glass is compositionally more complex than silica glass with the addition of other cations. These cations can be classified into two categories: the network formers like Ti, Al and network modifiers like Mg, Ca, Na and K. The two sets of cations have distinct effects on gas solubility. Network modifiers tend to form bonds between the bridging SiO_4 tetrahedra and lower the volume of void space. Their negative correlation with noble gas solubility has been experimentally observed (Tournour and Shelby, 2008a; Tournour and Shelby, 2008b). On the other hand, network formers, which reside in the Si site, seem to have less of an influence on gas solubility.

Geochemical Implications

The geometrical packing and coordination of atoms in silicate melts and glasses are similar at ambient and high pressure conditions based on experimental observations (Morard *et al.*, 2020;

Williams and Jeanloz, 1988). Hence, the void space distribution in melt structure is likely to be comparable and our results here support significant solubility of helium and neon in high pressure silicate melts (Fig. 3). Furthermore, the partition coefficients between mineral and melts for noble gases are in the order of 10^{-3} (Karato, 2016). It is expected silicate melts should be an important host for noble gases. He and Ne are the 2nd and 5th most abundant element in the solar system (Palme *et al.*, 2014). For $^{3}He/^{4}He$ and $^{20,21}Ne/^{22}Ne$ isotopic ratios, the discrepancy of upper mantle material value from atmospheric value has been a hot topic in geochemistry (e.g. Bekaert et al., 2019; Mukhopadhyay and Parai, 2019). Most answers to this question require a deep primordial reservoir which has unique geochemical features and survive mantle convection for the last 4.5 billion years. It has been noticed that some patches making of partially molten rock might exist at the core mantle boundary (e.g. Wen *et al.*, 2001). These melts may be able to host large amounts of noble gases like helium and neon with primordial and less-radiogenic features. Other than the core-mantle boundary, partial melting may also occur at the top of the lower mantle due to dehydration melting (Fu *et al.*, 2019). These layers might be perturbed by mantle convection more often and host noble gases with more radiogenic features. Therefore, the observed difference in noble gases ratios in OIBs and MORBs could be possibly due to sampling different melt reservoirs for noble gases. The storage of helium or neon discussed here reaches conditions beyond the range of this experiment, and due to the complex coordination environment change of silicon at higher pressures (Wang *et al.*, 2014), and the high temperature conditions in deep Earth, directly applying our results to these conditions may not be suitable. However, the mechanism revealed in this study and previous studies (Clark *et al.*, 2016; Sato *et al.*, 2011; Weigel *et al.*, 2012) (i.e., availability of interstitial void to compressed noble gases) is still valid and future structure simulation and void space analysis of heated silica/basalt glass at

high pressures is needed. Geodynamic simulations are also needed to better estimate the degree of mixing during these processes.

Noble gas-silicate interaction may also have important implications for the composition of the atmospheres of other planetary bodies like Jupiter. It is found that the abundances of helium and neon in Jupiter's atmosphere are significantly lower than other noble gases, when compared to solar composition (Fortney, 2010). Our results suggest that this discrepancy could be related to interior processes in the planet. Forming a He-Ne-silicate composite at Jupiter's rocky core could be a viable option. Whether such a mechanism could explain the deficit of neon and helium in Jupiter's atmosphere requires further experimental and computational work. Our study demonstrates the controlling factors for noble gas solubility in a silicate melt are the noble gas size compared to void size, indicating that data on the structure of silicate melts with natural compositions at higher *P-T* is crucially needed in order to estimate the storage capacity of noble gases in deep planetary interiors.

Acknowledgements

AEG and WM acknowledge support from NSF Geophysics (EAR0738873). Work was performed at GeoSoilEnviroCARS which is supported by NSF (EAR – 1634415) and DOE (DE-FG02-94ER14466). Use of the COMPRES-GSECARS gas loading system was supported by COMPRES under NSF (EAR -1606856) and GSECARS. The Advanced Photon Source is operated for the DOE Office of Science by Argonne National Laboratory (DE-AC02-06CH11357).

208

209 **References**

210 Angel, R.J., Bujak, M., Zhao, J., Gatta, G.D., Jacobsen, S.D. (2007) Effective hydrostatic limits
211 of pressure media for high-pressure crystallographic studies. *Journal of Applied*
212 *Crystallography* 40, 26–32.

213 Bajgain, S., Ghosh, D.B., Karki, B.B. (2015) Structure and density of basaltic melts at mantle
214 conditions from first-principles simulations. *Nature Communications* 6, 1–7.

215 Bekaert, D.V., Broadley, M.W., Caracausi, A., Marty, B. (2019) Novel insights into the
216 degassing history of Earth's mantle from high precision noble gas analysis of magmatic
217 gas. *Earth and Planetary Science Letters* 525, 115766.

218 Clark, A.N., Lesher, C.E., Jacobsen, S.D., Wang, Y. (2016) Anomalous density and elastic
219 properties of basalt at high pressure: Reevaluating of the effect of melt fraction on
220 seismic velocity in the Earth's crust and upper mantle. *Journal of Geophysical Research:*
221 *Solid Earth* 121, 4232–4248.

222 Fortney, J. (2010) Peering into Jupiter. *Physics* 3.

223 Fu, S. *et al.* (2019) Water Concentration in Single-Crystal (Al,Fe)-Bearing Bridgmanite Grown
224 From the Hydrous Melt: Implications for Dehydration Melting at the Topmost Lower
225 Mantle. *Geophysical Research Letters* 46, 10346–10357.

226 Guillot, B., Sator, N. (2007) A computer simulation study of natural silicate melts. Part II: High
227 pressure properties. *Geochimica et Cosmochimica Acta* 71, 4538–4556.

228 Karato, S. (2016) Physical basis of trace element partitioning: A review. *American Mineralogist*
229 101, 2577–2593.

230 Klotz, S., Chervin, J.C., Munsch, P., Lemarchand, G. (2009) Hydrostatic limits of 11 pressure
231 transmitting media. *Journal of Physics D Applied Physics* 42, 075413.

232 Liu, J., Lin, J.-F. (2014) Abnormal acoustic wave velocities in basaltic and (Fe,Al)-bearing
233 silicate glasses at high pressures. *Geophysical Research Letters* 41, 8832–8839.

234 Malavasi, G., Menziani, M.C., Pedone, A., Segre, U. (2006) Void size distribution in MD-
235 modelled silica glass structures. *Journal of Non-Crystalline Solids* 352, 285–296.

236 Morard, G. *et al.* (2020) In situ X-ray diffraction of silicate liquids and glasses under dynamic
237 and static compression to megabar pressures. *Proceedings of the National Academy of*
238 *Sciences*. National Academy of Sciences.

239 Mukhopadhyay, S., Parai, R. (2019) Noble Gases: A Record of Earth's Evolution and Mantle
240 Dynamics. *Annual Review of Earth and Planetary Sciences* 47, 389–419.

Murakami, M. (2018) Water makes glass elastically stiffer under high-pressure. *Scientific Reports* 8, 11890.

Palme, H., Lodders, K., Jones, A. (2014) Solar System Abundances of the Elements. *Treatise on Geochemistry*. Elsevier, 15–36.

Rosa, A.D., Bouhifd, M.A., Morard, G., Briggs, R., Garbarino, G., Irifune, T., Mathon, O., Pascarelli, S. (2020) Krypton storage capacity of the Earth's lower mantle. *Earth and Planetary Science Letters* 532, 116032.

Sakamaki, T., Kono, Y., Wang, Y., Park, C., Yu, T., Jing, Z., Shen, G. (2014) Contrasting sound velocity and intermediate-range structural order between polymerized and depolymerized silicate glasses under pressure. *Earth and Planetary Science Letters* 391, 288–295.

Salmon, P.S. *et al.* (2019) Pressure induced structural transformations in amorphous MgSiO3 and CaSiO3. *Journal of Non-Crystalline Solids: X* 3, 100024.

Sanchez-Valle, C., Bass, J.D. (2010) Elasticity and pressure-induced structural changes in vitreous MgSiO3-enstatite to lower mantle pressures. *Earth and Planetary Science Letters* 295, 523–530.

Sanloup, C., Schmidt, B.C., Perez, E.M.C., Jambon, A., Gregoryanz, E., Mezouar, M. (2005) Retention of Xenon in Quartz and Earth's Missing Xenon. *Science*. American Association for the Advancement of Science 310, 1174–1177.

Sato, T., Funamori, N., Yagi, T. (2011) Helium penetrates into silica glass and reduces its compressibility. *Nature Communications* 2, 345.

Shackelford, J.F., Masaryk, J.S. (1978) The interstitial structure of vitreous silica. *Journal of Non-Crystalline Solids* 30, 127–134.

Shen, G., Mei, Q., Prakapenka, V.B., Lazor, P., Sinogeikin, S., Meng, Y., Park, C. (2011) Effect of helium on structure and compression behavior of SiO2 glass. *Proceedings of the National Academy of Sciences* 108, 6004–6007.

Tournour, C.C., Shelby, J.E. (2008a) Neon solubility in silicate glasses and melts. *Physics and Chemistry of Glasses* 49, 8.

Tournour, C.C., Shelby, J.E. (2008b) Helium solubility in alkali silicate glasses and melts. *Physics and Chemistry of Glasses - European Journal of Glass Science andTechnology Part B* 49, 207–215.

Wang, Y. *et al.* (2014) Atomistic insight into viscosity and density of silicate melts under pressure. *Nature Communications* 5, 3241.

Weigel, C., Polian, A., Kint, M., Rufflé, B., Foret, M., Vacher, R. (2012) Vitreous Silica Distends in Helium Gas: Acoustic Versus Static Compressibilities. *Physical Review Letters* 109, 245504.

Wen, L., Silver, P.G., James, D.E., Kuehnel, R. (2001) Seismic evidence for a thermo-chemical boundary at the base of the Earth's mantle. *Earth and Planetary Science Letters* 189, 141–153.

Williams, Q., Jeanloz, R. (1988) Spectroscopic Evidence for Pressure-Induced Coordination Changes in Silicate Glasses and Melts. *Science*. American Association for the Advancement of Science 239, 902–905.

Zha, C., Hemley, R.J., Mao, H., Duffy, T.S., Meade, C. (1994) Acoustic velocities and refractive index of SiO2 glass to 57.5 GPa by Brillouin scattering. *Physical Review B* 50, 13105–13112.

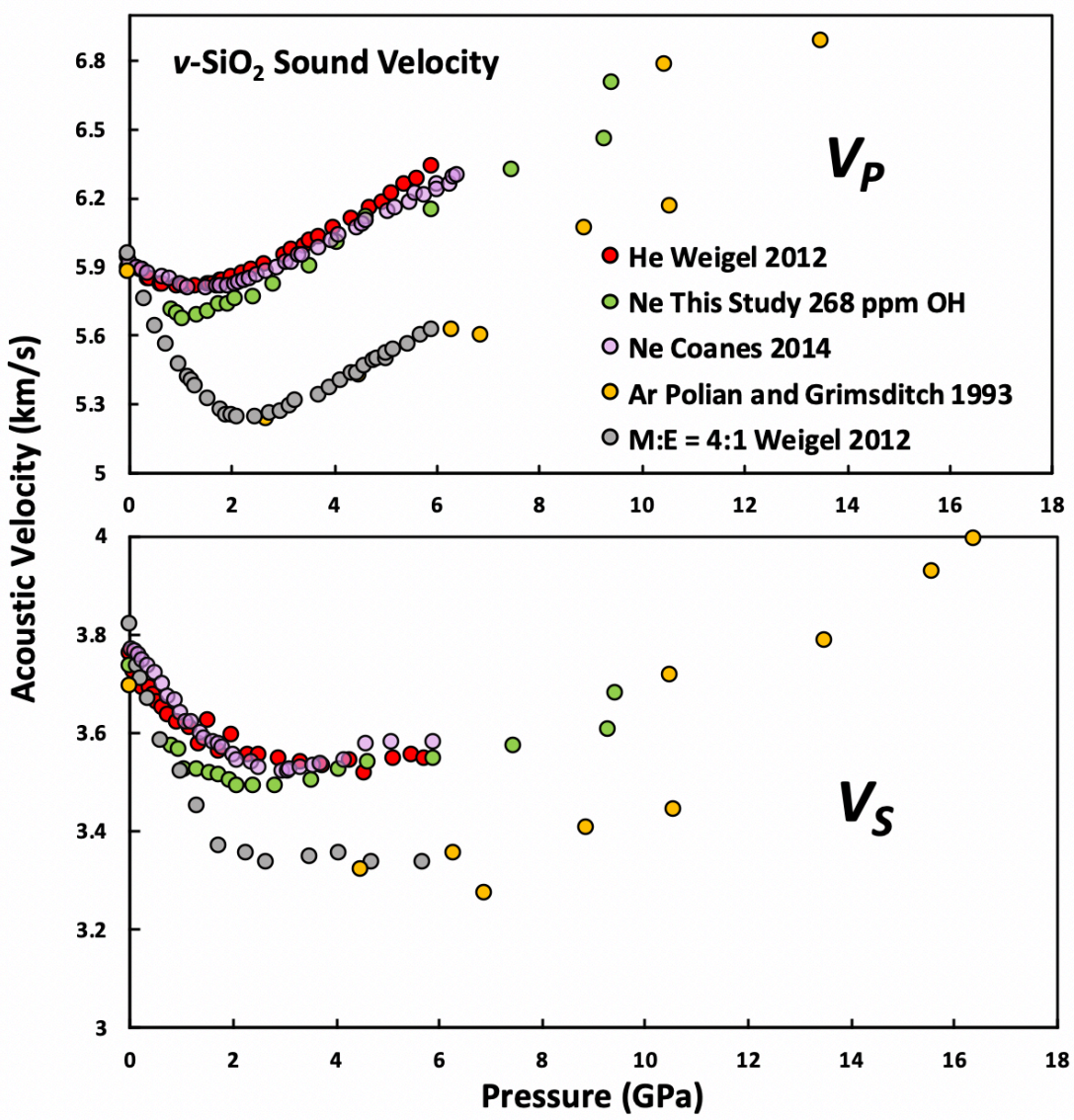

Figure 1. Sound velocities of vitreous silica under high pressure in different pressure media. M-E represents 4:1 Methanol-Ethanol mixture. Errors of the velocities are estimated from statistical uncertainties arising from the peak fitting. Typical errors are less than 1.5 % and smaller than the size of the symbols. For both the V_P and V_S of silica in different noble gas media, we found a consistent trend for the acoustic velocities—He>Ne>Ar≈M-E. The abnormal velocity minimum at around 2-5 GPa can be attributed to the rearrangement of SiO_4 tetrahedra in the vitreous silica structure (Clark et al., 2016).

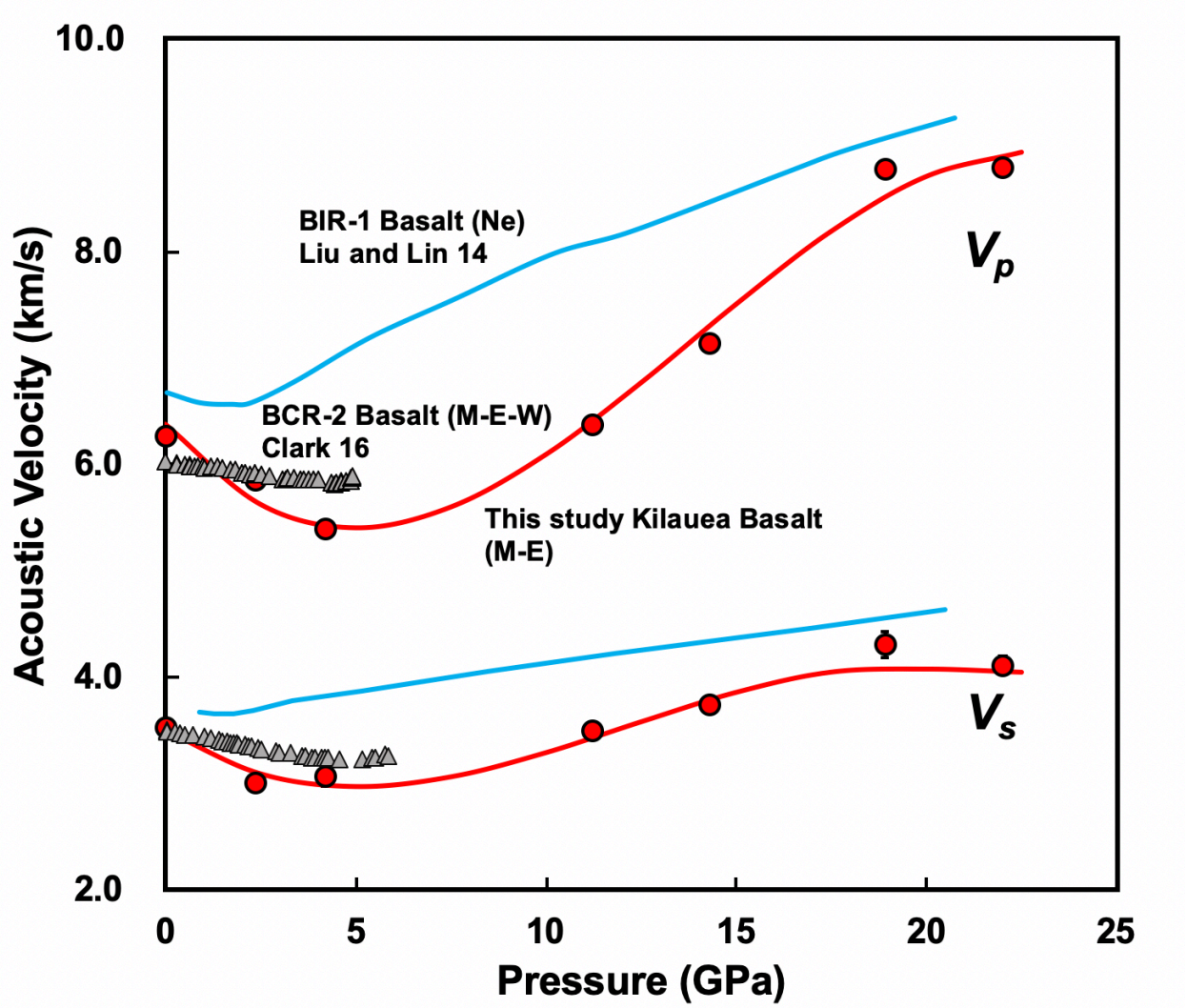

Figure 2. Sound velocities of basalt glasses at high pressure. M-E-W: 16:3:1 Methanol-Ethanol-Water mixture, M-E: 4:1 Methanol-Ethanol mixture. Errors of the velocities are estimated from statistical uncertainties arising from the peak fitting. Error bars smaller than the symbols plotted are not shown. Although the three basalt glasses have slightly different composition, their degrees of polymerization (NBO/T= 0.6, 0.9 and 0.8 for BCR-2, BIR-1 and KB, respectively) are quite similar (BIR-1, blue colored line, Liu and Lin, 2014; BCR-2, triangular points, Clark et al., 2016). The extents of the velocity drops are very different among the glasses. We observed that BIR-1 has a 2 % drop for both V_P and V_S, BCR-2 has a 2.8 % drop for V_P and a 7.2 % drop for V_S, while KB in M-E has a 14 % drop for both V_P and V_S. We attribute this variation to be mostly due to the different pressure media used. H_2O and Ne have relatively small molecule size that can possibly penetrate into the structure of silicate glass and make it stiffer (Fig. 3 and S-4).

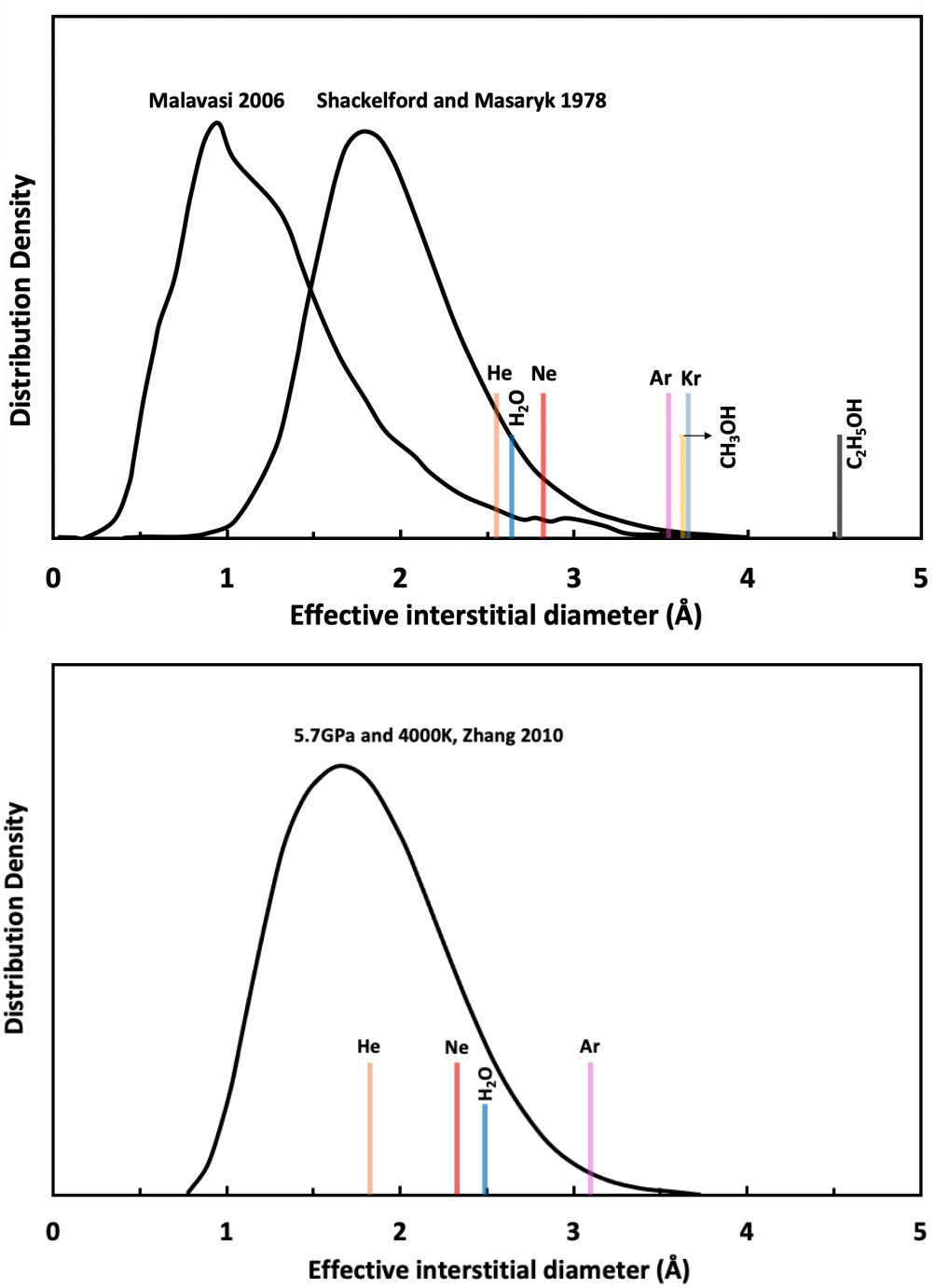

Figure 3. Void size distribution of SiO_2 and molecular size of common pressure media at ambient condition and high pressure. Top panel: Molecular size data at ambient conditions were adapted from Reid et al., 1987. Bottom panel: High pressure molecule sizes were calculated using equations of state (He: Loubeyre et al., 1993; Ne: Dewaele et al., 2008; Ar: Ross et al., 1986, H_2O: Yoshimura et al., 2006).

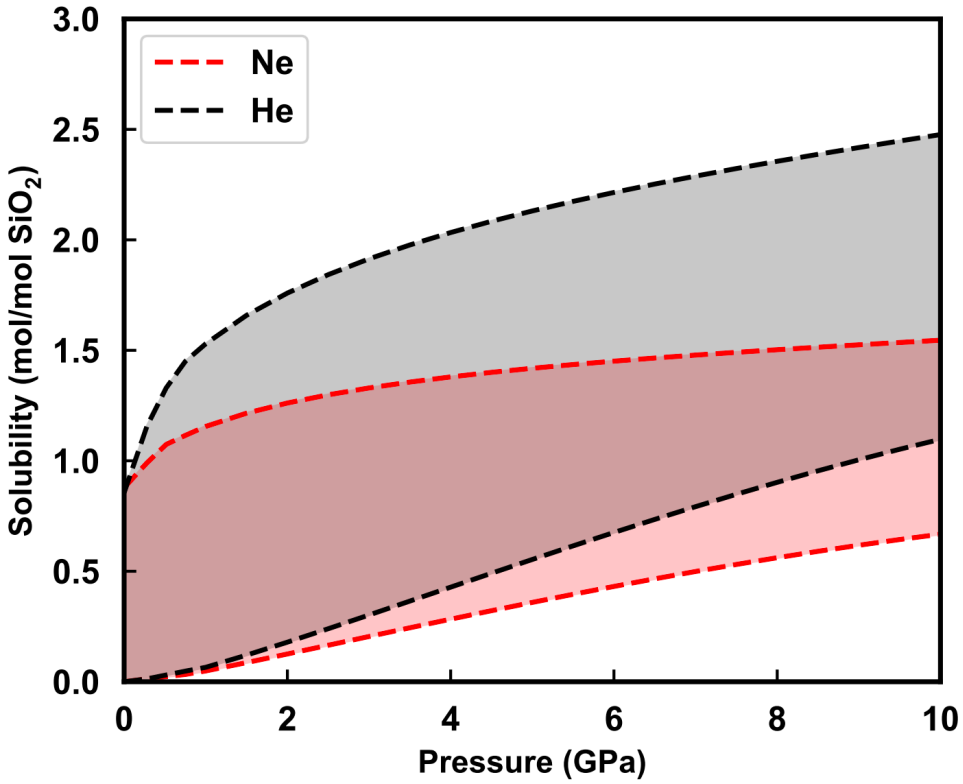

Figure 4. Solubility of neon and helium in vitreous silica at high pressure. The two lines for each medium represent upper limit and lower limit, respectively. The lower and upper limits were estimated by $(V_{rigid}-V_{normal})/V_{gas}$ and $(V_{rigid}-V_{sixfold})/V_{gas}$, respectively, where V_{rigid} and V_{normal} represent the molar volume of SiO_2 glass in noble gas media and non-gas media conditions, accordingly; V_{gas} – the molar volume of noble gas; $V_{sixfold}$ – the molar volume of sixfold-coordinated SiO_2 glass (Sato et al., 2011). We do not have an accurate determination of volume of silica in Ne, instead we assume the volume change under pressure is same as the He case, as similar volume curves were suggested by integration method (Fig. S-3).